Basic scattering methods for radiative transfer simulations

Meng Gao*, Ping Yang and George Kattawar
Texas A&M University, 05/23/2014
(*now at SSAI, NASA GSFC)

Introduction

Radiative transfer simulation is fundamental for the study of energy budget in atmospheric and oceanic system. It is also the core for the satellite remote sensing applications. The simulations require the knowledge of the single scattering properties from individual particles, and can provide the diffuse reflected and transmitted radiance from the multiple scattering among a collection of the particles. In this report, we discuss the basic concepts and numerical simulation methods for both single and multiple scattering methods including the 2D geometrical ray tracing method, and the Monte Carlo radiative transfer method. The Monte Carlo code is also extended to discuss the method of sucessive orders of scattering (SOS). The numerical source codes and examples are implemented and provided for all the methods discussed in this report. The readers are encouraged to modify and experiment with the numerical codes to explore the underlying law that governs the nature of light scattering.

2D Geometrical Ray Tracing

For small size particles (size parameter less than the order of 10), the numerically accurate methods, such as Discrete Dipole Approximation (DDA) method, and Finite Difference Time Domain (FDTD) method, are efficient to study the single scattering properties, such as the scattering phase function and the scattering and absorption cross section. For particles with large sizes, both DDA and FDTD become impractical with respect to the requirement of computational resources. But the ray tracing method based on geometrical optics become efficient and accurate in calculating the scattering properties. In the ray tracing process as shown in the example of a sphere (Figure 1), a ray is incident on the particle from an arbitrary direction, and is split into the reflected and refracted rays. The refracted ray exits the particle and its intensity will be accumulated in a detector along the

scattering direction. The reflected ray will continue propagating until its intensity become negligible, and then a new ray will be generated with a random incident direction. After a large amount of rays are simulated, the phase function is obtained from the intensity accumulated in each scattering direction. The ray tracing process of a convex geometric object can be achieved following a similar algorithm.

Upon the ray interact with an interface, the reflectance and transmittance determine how much energy from the incoming light is reflected or transmitted through the interface. The reflection and transmission of the electric field at a dielectric interface is solved using the boundary conditions of the Maxwell equations, and are summarized in the following Fresnel Formulas (Born and Wolf 1999). The reflection and transmission for the parallel (p) and perpendicular(s) electric field components can be represented as:

$$r_p = \frac{\tan(\theta_i - \theta_t)}{\tan(\theta_i + \theta_t)}, \tag{1}$$

$$r_s = -\frac{\sin(\theta_i - \theta_t)}{\sin(\theta_i + \theta_t)}, \tag{2}$$

$$t_p = \frac{2\sin\theta_t \cos\theta_i}{\sin(\theta_i + \theta_t)\cos(\theta_i - \theta_t)}, \tag{3}$$

$$t_s = \frac{2\sin\theta_t \cos\theta_i}{\sin(\theta_i + \theta_t)}, \tag{4}$$

and the incident angle and the refracted angle are associated from the Snel's law of refraction,

$$\frac{\sin\theta_i}{\sin\theta_t} = \frac{n_2}{n_1}, \tag{5}$$

where θ_i is the incident angle in medium 1 with a refractive index n_1, and θ_t is the refracted angle in medium 2 with a refractive index n_2. When absorption in the particle is present, an adjusted refractive index is introduced in order to conduct correct ray tracings. More detailed algorithms are reviewed by Yang et al (Yang and Liou 1995).

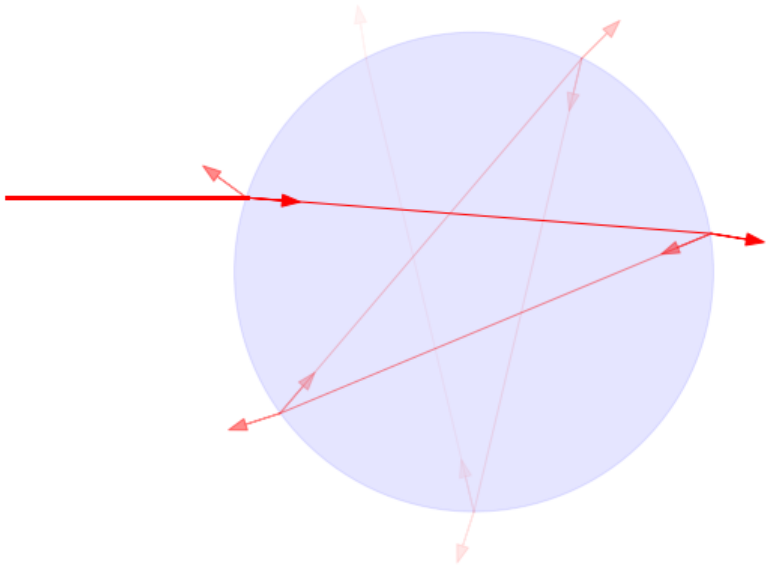

Figure 1. A ray is incident on a sphere, after each reflection and transmission its intensity decreases. Note the opacity of the ray is not linearly scaled with the intensity.

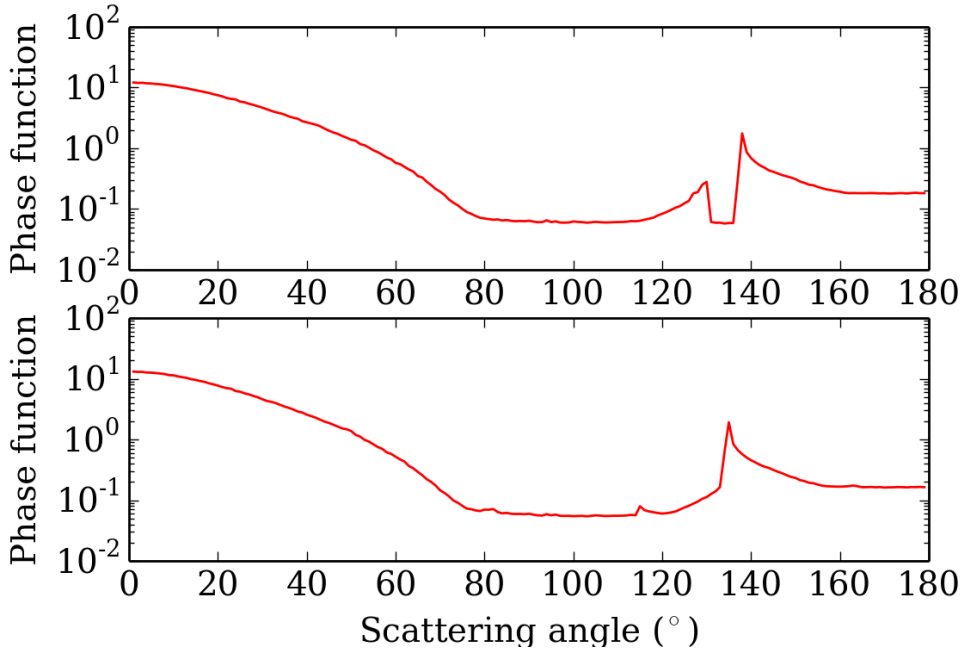

Figure 2. Phase functions from 2D ray tracing of a sphere with a refractive index of $n = 1.33$ *(upper panel) and* $n = 1.31$ *(lower panel).*

As an example shown in Figure 2, the phase functions of spheres are calculated for two different refractive indices, $n = 1.33$ and $n = 1.31$ respectively. The medium has a unitary refractive index. The phase functions calculated from the 2D ray tracing method only depend on the value of the refractive index and the geometry of the particle. For the sphere with $n = 1.33$, two scattering peaks around 130° are prominent and are corresponding to the primary and secondary rainbows. When $n = 1.31$ only one scattering peak is visible.

Efficient Monte Carlo Radiative Transfer Simulation

A turbid medium includes a collection of particles randomly positioned and oriented. If the particles are well separated, only incoherent scattering is important. The incident light will be scattered multiple times by the scatterers in the medium before leaving the system, and radiance in the turbid medium is governed by the radiative transfer equation (Chandrasekhar 2011). As a versatile method, the Monte Carlo method treat the incident light as a collection of photon package, and each photon has an initial unitary weight. The photon will propagate in the medium and be scattered by

the particles. The propagating distance and scattering directions are statistically sampled based on the single scattering properties of the particles.

Traditional Monte Carlo method will discard each photon when it excape the system, and therefore has low efficient to achieve enough accuracy. In our algorithm several variance reduction methods are implemented to increate the efficiency and accuracy, for example the forced collision algorithm is used to sample the optical depth and the estimation scheme is used to calculate the phase function. The forced collision method samples the optical depth that a photon propagates in the medium by

$$\tau' = -ln(1-[1-\exp(-\tau)]\zeta) \ , \tag{6}$$

where ζ is a uniformly distributed random number over [0, 1] and τ is the optical depth along the photon path. In this way, the sampled optical depth τ' is always within the system, and therefore no photon can escape. The estimation scheme can increate the simulation efficiency but estimate the contribution of a virtual photon to each detectors without really propagating the photon (Zhai, Kattawar et al. 2008).

In the example provided in the source code, a Rayleigh scattering particle is implemented in the medium. The Rayleigh phase function has a simple form

$$P(\theta) = \frac{3}{16\pi}(1+\cos^2\theta), \tag{7}$$

The scattering angle θ can be sampled according to the phase function. The code can be extended to include other types of particles by modifying the sampling subroutine for the scattering angles. As shown in Figure 3, by increasing the optical depth of the system, the reflected (zenith angle from 0° to 90°) and transmitted (zenith angle from 90° to 180°) diffuse radiance become more and more diffuse. A thorough discussion on how the angular distribution of the diffuse reflection depends on the optical depth can be found in Gao et al (Gao, Huang et al. 2013).

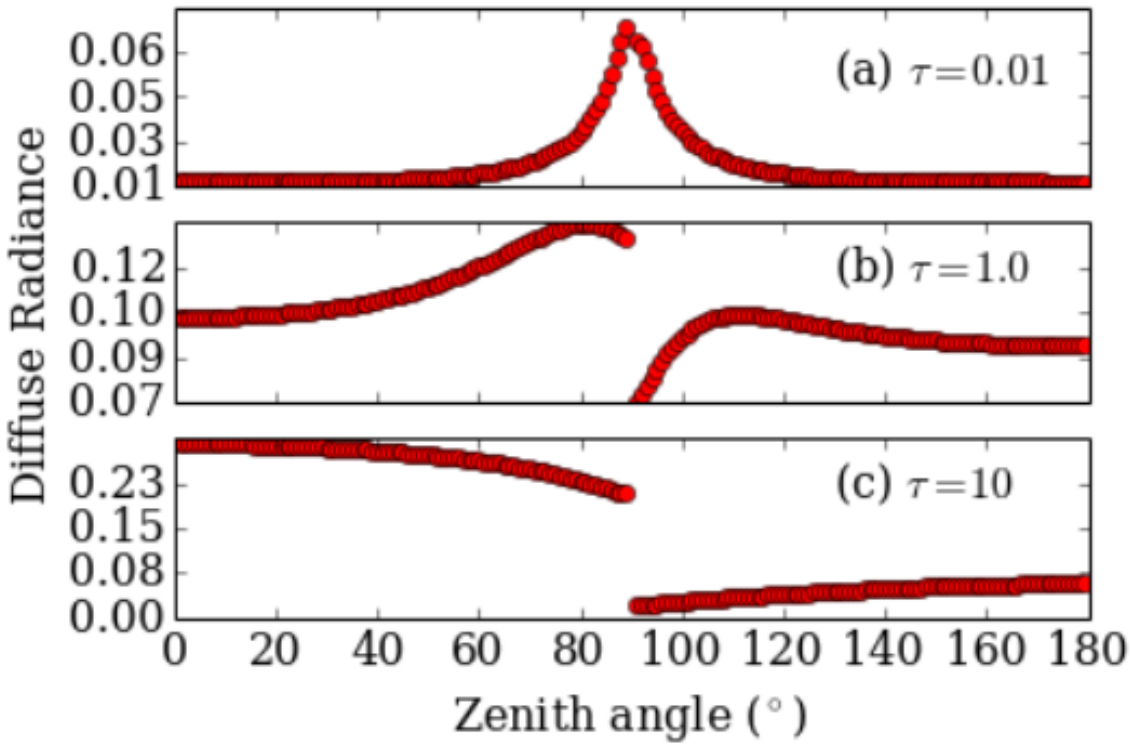

Figure 3. The diffuse radiance in a Rayleigh scattering plane parallel system with a normal optical depth τ *=0.01, 1.0 and 10. The reflected radiance is for the zenith angle from* 0° *to* 90° *and transmitted radiance is for the zenith angle from* 90° *to* 180°.

Successive Order of Scattering (SOS)

During the radiative transfer process as discussed from the Monte Carlo simulation, each photon can be scattered several times before its weight become negligible. Therefore the solution of the radiative transfer theory can be organized as the summation of various terms and each term corresponds to a different order of scattering (Wendisch and Yang 2012).

The first order of scattering can be derived analytically for arbitrary incident directions and system optical depths as

$$I_r = \frac{|\mu_0| F_0}{|\mu| + |\mu_0|} \mathbf{P}(\Omega, \Omega_0)[1 - \exp(-\frac{|\mu| + |\mu_0|}{|\mu||\mu_0|}\tau)], \qquad (8)$$

$$I_t = \frac{|\mu_0| F_0}{|\mu_0| - |\mu|} \mathbf{P}(\Omega, \Omega_0)[\exp(-\tau_m / |\mu_0|) - \exp(-\tau / |\mu|)], \quad (9)$$

where I_r and I_t are the diffuse radiance for the reflection and transmission, $\mathbf{P}(\Omega, \Omega_0)$ is the phase function for incident direction Ω_0 and scattered direction Ω, τ is the optical depth of the system, $\mu_0 = \cos\theta_0$ is the cosine of the incident zenith angle and $\mu = \cos\theta$ is the cosine of the scattering zenith angle, and F_0 is the incident irradiance. The incident irradiance is chosen as one.

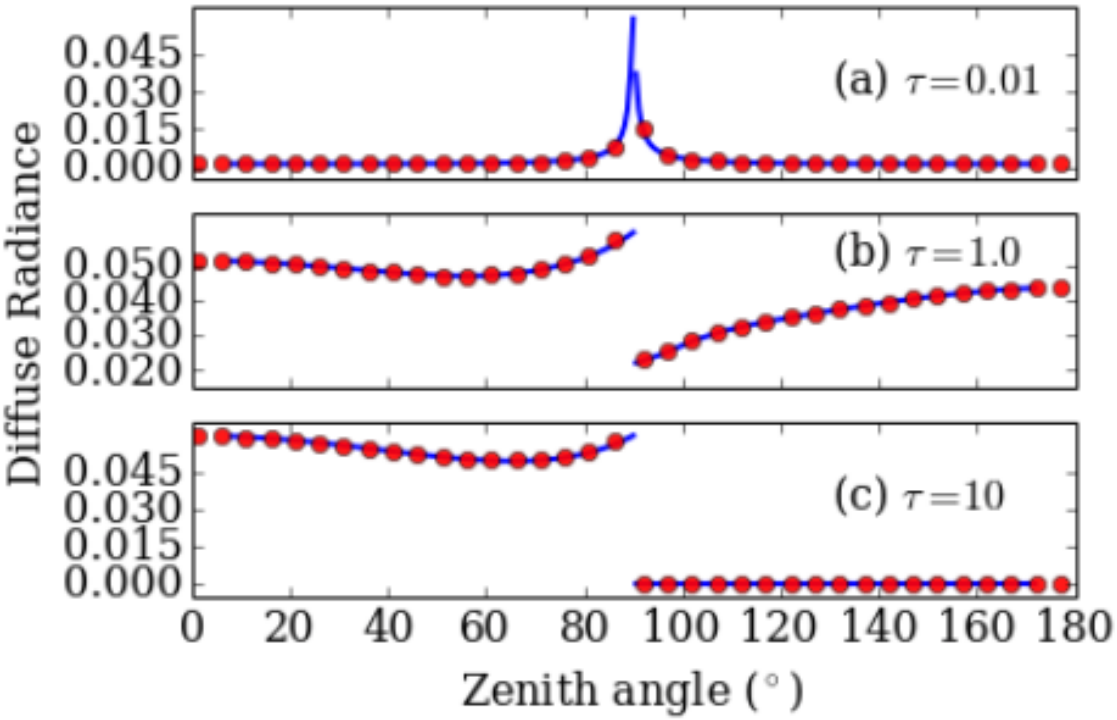

Figure 4. Single scattering approximations for a turbid medium with different optical depth τ. Solid line is the analytical results, and the red dots are the Monte Carlo simulation for the first order of scattering in a Rayleigh scattering medium with $\tau = 0.01$ (a), $\tau = 1.0$ (b) and $\tau = 10$ (c), and normal incidence.

For higher order terms, the mathematical expression can be very complex. It is convenient to calculate the contribution of each term using the Monte Carlo simulation. The aforementioned Monte Carlo code is modified by setting a constraint on the number of scattering for each photon. In the case of a Rayleigh scattering medium with a beam of light incident in the normal direction, the simulation results are summarized in Figures 4 and 5. Figure 4

shows the simulated results match well with the analytical results form Eqs (8) and (9). When the optical depth is small, such as $\tau = 0.01$, the first order of scattering dominates in the solution, and there is a peak around the scattering direction close to horizon. As shown in Figure 5 for a medium with $\tau = 1$, by including more orders of scatterings, the radiance approaches to the exact solution. Although the medium has only an optical depth of 1, namely the physical depth equals to one mean free path, but higher order scattering terms are still important in predicting the correct diffuse radiance.

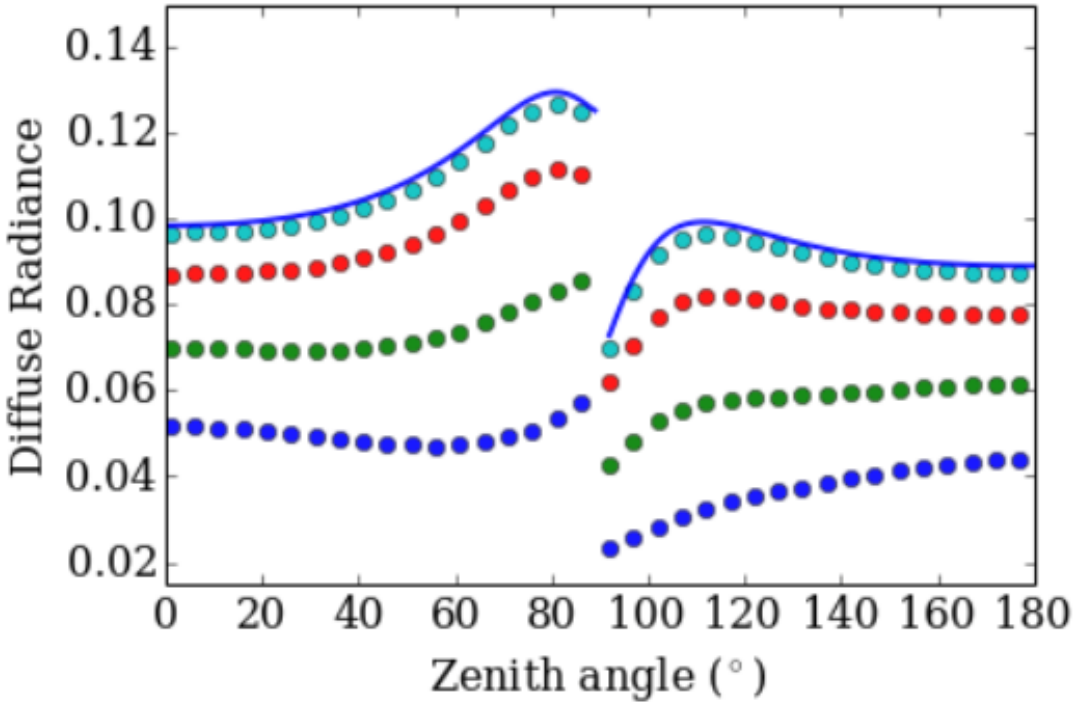

Figure 5. The diffuse radiance contributed from the first 1, 2, 4, 8 orders of scattering (corresponding to the dot plot upward from bottom) for a turbid medium with an optical depth 1. The solid line is the radiance from all orders of scatterings.

Conclusions

We have summarized several numerical methods for the light scattering simulations including the geometrical ray tracing method, Monte Carlo radiative transfer method, and the successive order of scattering methods. Each method emphasizes different aspects of the physics and concept associated with the single and multiple scattering processes thus provides a basis for the study of radiative transfer. The corresponding numerical codes

and examples are also provided. All the data and graphs discussed in this report are produced through the codes distributed together with this document.

Reference

Born, M. and E. Wolf (1999). Principles of Optics: Electromagnetic Theory of Propagation, Interference and Diffraction of Light.

Chandrasekhar, S. (2011). Radiative Transfer, Dover Publications, Inc.

Gao, M., X. Huang, P. Yang and G. W. Kattawar (2013). "Angular distribution of diffuse reflectance from incoherent multiple scattering in turbid media." Applied Optics **52**(24): 5869-5879.

Wendisch, M. and P. Yang (2012). Theory of Atmospheric Radiative Transfer.

Yang, P. and K. N. Liou (1995). "Light scattering by hexagonal ice crystals: comparison of finite-difference time domain and geometric optics models." Journal of the Optical Society of America A **12**(1): 162-176.

Zhai, P.-W., G. W. Kattawar and P. Yang (2008). "Impulse response solution to the three-dimensional vector radiative transfer equation in atmosphere-ocean systems. I. Monte Carlo method." Applied Optics **47**(8): 1037-1047.